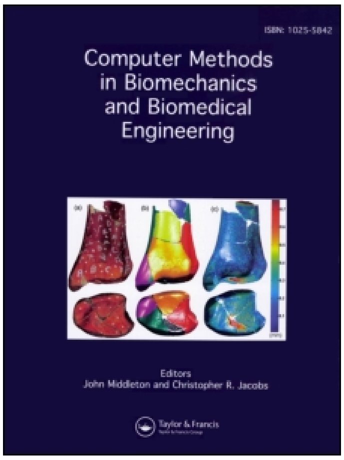

Computer Methods in Biomechanics and Biomedical Engineering
Publication details, including instructions for authors and subscription information:
http://www.informaworld.com/smpp/title~content=t713455284

Estimates of muscle function in human gait depend on how foot-ground contact is modelled

Tim W. Dorn[a]; Yi-Chung Lin[a]; Marcus G. Pandy[a]
[a] Department of Mechanical Engineering, University of Melbourne, Melbourne, Victoria, Australia

First published on: 24 May 2011

To cite this Article Dorn, Tim W. , Lin, Yi-Chung and Pandy, Marcus G.(2011) 'Estimates of muscle function in human gait depend on how foot-ground contact is modelled', Computer Methods in Biomechanics and Biomedical Engineering,, First published on: 24 May 2011 (iFirst)

To link to this Article: DOI: 10.1080/10255842.2011.554413

URL: http://dx.doi.org/10.1080/10255842.2011.554413

Computer Methods in Biomechanics and Biomedical Engineering
iFirst article, 2011, 1–12

Estimates of muscle function in human gait depend on how foot-ground contact is modelled

Tim W. Dorn*, Yi-Chung Lin and Marcus G. Pandy

Department of Mechanical Engineering, University of Melbourne, Melbourne, Victoria 3010, Australia

(*Received 25 October 2010; final version received 10 January 2011*)

Computational analyses of leg-muscle function in human locomotion commonly assume that contact between the foot and the ground occurs at discrete points on the sole of the foot. Kinematic constraints acting at these contact points restrict the motion of the foot and, therefore, alter model calculations of muscle function. The aim of this study was to evaluate how predictions of muscle function obtained from musculoskeletal models are influenced by the model used to simulate ground contact. Both single- and multiple-point contact models were evaluated. Muscle function during walking and running was determined by quantifying the contributions of individual muscles to the vertical, fore-aft and mediolateral components of the ground reaction force (GRF). The results showed that two factors – the number of foot-ground contact points assumed in the model and the type of kinematic constraint enforced at each point – affect the model predictions of muscle coordination. Whereas single- and multiple-point contact models produced similar predictions of muscle function in the sagittal plane, inconsistent results were obtained in the mediolateral direction. Kinematic constraints applied in the sagittal plane altered the model predictions of muscle contributions to the vertical and fore-aft GRFs, while constraints applied in the frontal plane altered the calculations of muscle contributions to the mediolateral GRF. The results illustrate the sensitivity of calculations of muscle coordination to the model used to simulate foot-ground contact.

Keywords: locomotion biomechanics; musculoskeletal; ground reaction force; centre of mass; multi-joint coordination; induced accelerations

Introduction

A muscle can exert a torque about a joint only if it spans that joint. However, a muscle can simultaneously accelerate all the joints in the body, even those not spanned by the muscle. This is a consequence of dynamic coupling, whereby the force applied by a muscle is transmitted through the bones to all the joints in the body (Zajac and Gordon 1989). If a muscle force contributes to the accelerations of all the joints, then it also must contribute to the acceleration of the body's centre of mass and hence, by Newton's second law of motion (i.e. force equals mass times acceleration), to the force exerted on the ground. Thus, the functional role of a muscle may be determined by quantifying its contribution to the ground reaction force (GRF).

A number of studies have described leg-muscle function during gait by calculating the contributions of individual muscles to the accelerations of the lower-limb joints (Kepple et al. 1997a; Arnold et al. 2005; Goldberg and Kepple 2009) and to the acceleration of the body's centre of mass (Kepple et al. 1997b; Anderson and Pandy 2003; Sasaki and Neptune 2006; Liu et al. 2008; Xiao and Higginson 2008; Hamner et al. 2010; Pandy et al. 2010). In each of these studies, a simplified model of ground contact was used to simulate the dynamic interaction between the foot and the ground. These simplified models often assume that foot-ground contact occurs at discrete points which vary in number from a single point located at the centre of pressure (CoP) (Kepple et al. 1997b; Liu et al. 2008; Goldberg and Kepple 2009; Hamner et al. 2010) to multiple points distributed over the sole of the foot (Neptune et al. 2000; Anderson and Pandy 2003; Pandy et al. 2010). At each contact point, kinematic constraints are applied, either explicitly as hard constraints (Kepple et al. 1997b; Anderson and Pandy 2003; Hamner et al. 2010; Pandy et al. 2010) or implicitly by using springs and dampers to simulate the interaction between the foot and the ground (Sasaki and Neptune 2006; Liu et al. 2008). Kinematic constraints alter the motion of the foot and, therefore, potentially influence the model calculations of muscle function.

Models of ground contact should include the effects of impact, friction and distributed contact, all of which are manifested as kinematic constraints. Unfortunately, the effects of these kinematic constraints cannot be directly measured, and so model predictions of muscle function cannot be rigorously validated. However, a theoretical principle called 'superposition' may be used to gain confidence in the model predictions (Anderson and Pandy 2003; Hamner et al. 2010; Lin et al. 2011; Pandy et al. 2010). This principle states that the sum of the contributions of all action forces (e.g. muscles, gravity

*Corresponding author. Email: t.dorn@pgrad.unimelb.edu.au

ISSN 1025-5842 print/ISSN 1476-8259 online

DOI: 10.1080/10255842.2011.554413
http://www.informaworld.com

Table 1. Summary of the six ground-contact models evaluated in this study. X, Y and Z define, respectively, the fore-aft, vertical and mediolateral axes of the foot segment in the model.

	Ground-contact model	Contact location	Kinematic constraints		Degrees of freedom	Reference
			Linear [X Y Z]	Rotational [X Y Z]		
Time-independent	BALL	CoP	[1 1 1]	[0 0 0]	3	Kepple et al. (1997b)
	UNIVERSAL	CoP	[1 1 1]	[0 1 0]	2	Hamner et al. (2010)
	HINGE	CoP	[1 1 1]	[1 1 0]	1	*Goldberg and Kepple (2009)
	WELD	CoP	[1 1 1]	[1 1 1]	0	Kepple et al. (1997a)
Time-dependent	SINGLEPOINT	CoP	[1 1 1]	f(CoP)	f(CoP)	**Liu et al. (2008)
	MULTIPOINT	5 Points	f(CoP)	N/A	f(CoP)	Anderson and Pandy (2003) Arnold et al. (2005) Pandy et al. (2010)

Kinematic constraints applied at each foot-contact point were weighted between 0 and 1, where 0 represented an unconstrained degree-of-freedom, and 1 represented a fully constrained degree-of-freedom. In four of the models (BALL, UNIVERSAL, HINGE and WELD) time-independent kinematic constraints were applied at a single point under the foot: the CoP. The BALL contact model allowed rotations about all three joint axes; the UNIVERSAL model allowed rotations about the fore-aft and mediolateral joint axes; the HINGE model allowed rotations about the mediolateral joint axis; and the WELD model did not permit any relative movement between the foot and the ground. Linear motion of the CoP was always fully constrained for each time-independent contact model. In the remaining two models (SINGLEPOINT and MULTIPOINT) time-dependent constraints were applied at each foot-contact point as a function of the location of the foot CoP, indicated by f(CoP) (see Figure 1). Where possible, contact models used in previous studies were matched to the set of contact models used in this study.

* Goldberg and Kepple (2009) prescribed a WELD constraint in the small amount of time between foot-flat and heel-off, and a HINGE constraint for the remainder of the gait cycle.

** Liu et al. (2008) determined the rotational kinematic constraints not as a function of CoP, but rather as an explicit function of time. From foot-flat to heel-off, rotational $[X, Y, Z] = [1\ 1\ 1]$, at all other times rotational $[X, Y, Z] = [0, 0, 0]$. Weightings were modulated using a smooth ‘falloff’ function.

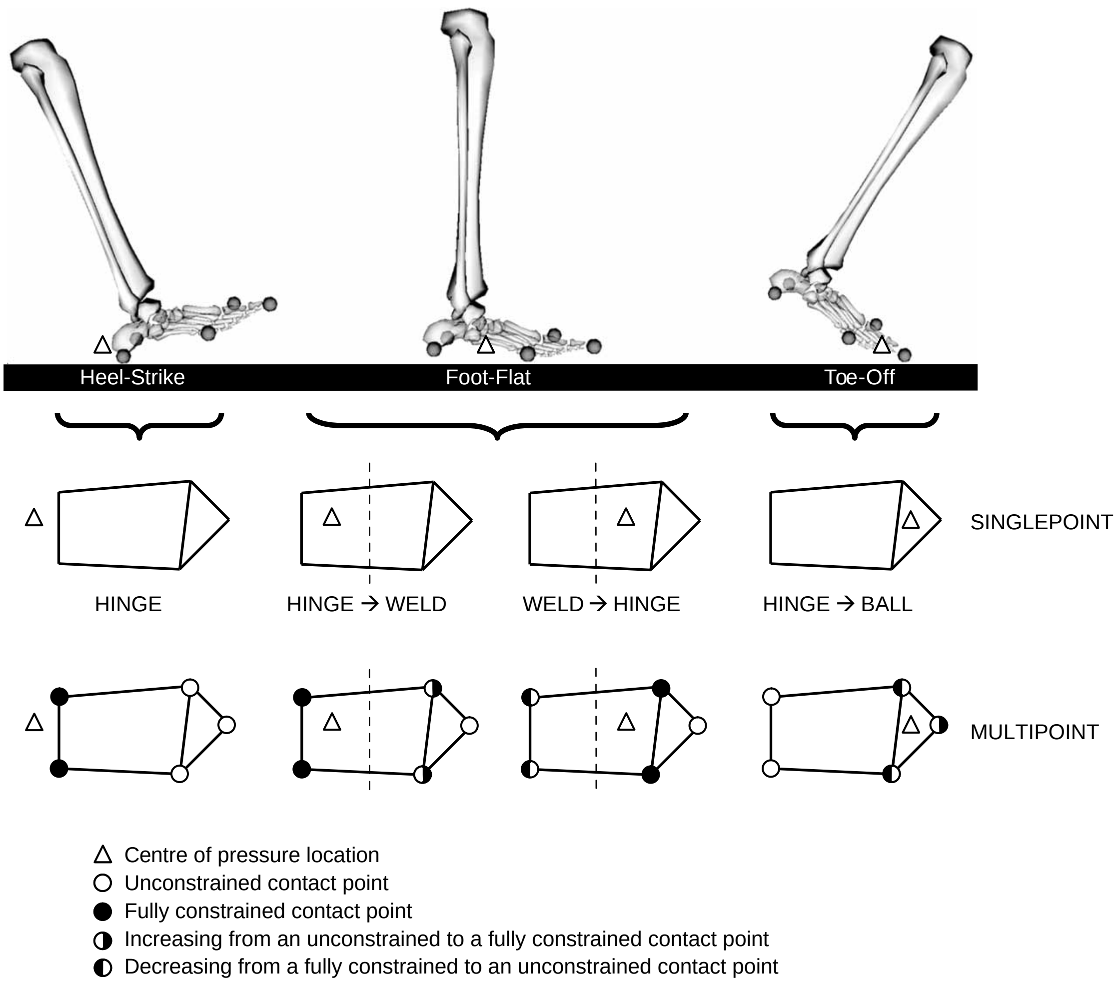

Figure 1. Diagram illustrating how the time-dependent kinematic constraints applied at the foot-contact points varied as a function of the location of the foot centre-of-pressure in the SINGLEPOINT and MULTIPOINT models. In the SINGLEPOINT model, contact occurred at the CoP and the constraints transitioned from the HINGE at heel strike to the WELD at midstance, and finally to the BALL at toe-off. In the MULTIPOINT model, contact occurred at five discrete points distributed over the foot. Weighting coefficients ranging from 0 to 1 were applied at each contact point to allow the foot to transition smoothly from heel-strike to foot-flat and from foot-flat to toe-off (see Table 1).

and centrifugal forces) to the GRF must be equal to the total GRF measured in a gait experiment. Although superposition is a necessary condition for evaluating the accuracy of the model calculations of muscle function, it is not sufficient for determining the validity of the individual contributions of the various action forces to the total GRF. Results obtained from a given model of ground contact may, therefore, satisfy superposition and still yield erroneous estimates of muscle function.

The overall goal of this study was to evaluate how calculations of muscle function are influenced by the model used to simulate foot-ground contact. Our specific aim was to determine the effects of kinematic constraints and the number of foot-ground contact points on calculations of muscle contributions to the GRF in walking and running.

Methods

Overground gait experiments were performed on 14 healthy adults (age, 28.5 ± 8.3 years; weight, 71.2 ± 8.0 kg; height, 176.2 ± 5.8 cm) as each subject walked and ran at their preferred speeds (walking: $n = 13$, 1.46 ± 0.11 m/s; running: $n = 10$, 3.42 ± 0.13 m/s). Experiments were conducted in the Human Motion Laboratory at the University of Melbourne and in the Biomechanics Laboratory at the Australian Institute of Sport. Subjects gave their informed consent after approval was obtained from the relevant institutional Human Research Ethics Committees.

Reflective markers were mounted over anatomical landmarks on the trunk and lower limbs of each subject. Kinematic data were acquired using a three-dimensional video motion capture system (VICON, Oxford Metrics, UK).

GRFs were measured simultaneously using a series of force plates embedded in the ground. In all trials, subjects made initial ground contact with their heels. Surface electromyographic (EMG) electrodes were placed over the bellies of six muscles in one leg: gluteus maximus, gluteus medius, medial hamstrings, vastus lateralis, medial gastrocnemius and soleus. The raw EMG signal was passed through a Teager–Kaiser energy filter to improve onset detection (Li et al. 2007). Marker trajectories were low-pass filtered using a fourth-order Butterworth filter with a cut-off frequency of 4 Hz. A Gait-Extract toolbox developed in MATLAB (freely available from https://simtk.org/home/c3dtoolbox/) was used to extract and process the raw marker trajectories, GRFs and EMG data for input into the musculoskeletal model.

The musculoskeletal model used in this study was identical to that described by Anderson and Pandy (1999). The skeleton was represented as a 10-segment, 23-degree-of-freedom mechanical linkage. The pelvis was free to translate and rotate in space. The head, arms and torso were lumped together as a single rigid body, which articulated with the pelvis via a ball-and-socket back joint. Each hip was modelled as a ball-and-socket joint, each knee as a hinge joint, each ankle-subtalar complex as a universal joint and each metatarsal as a hinge joint. The skeleton was actuated by 54 muscle-tendon units, each unit represented as a Hill-type muscle in series with an elastic tendon.

Subject-specific models of the skeleton were generated by scaling the anthropometric properties of each segment according to each subject's height and weight. Joint-centre locations and joint axes of rotation were determined by minimising the differences between measured and model-computed marker positions during isolated joint motion trials (Reinbolt et al. 2005; Kim et al. 2009). Force generating properties, attachment sites and the paths of all muscles in the model were the same as those identified by Anderson and Pandy (1999).

Inverse dynamics and optimisation theory were used to calculate leg-muscle forces for walking and running. Joint kinematics and GRFs were input into the model skeleton to calculate the net joint moments exerted about the back, hip, knee, ankle and metatarsal joints. At each time instant, the net joint moments were decomposed into individual muscle forces by solving an optimisation problem that minimised the sum of the squares of the muscle activations subject to physiological bounds imposed by each muscle's force-length-velocity property (Anderson and Pandy 2001b).

Six different ground-contact models were evaluated in this study. These models were selected because they have been implemented in previous studies reported in the literature (see Table 1). Each contact model differed by either the number of contact points defined on the sole of the foot or the type of kinematic constraint enforced at each foot-contact point. Kinematic constraints were defined by specifying a set of weighting coefficients associated with the linear and/or rotational degrees of freedom permitted at each contact point. The value of each weighting coefficient ranged from 0 to 1, where 0 denoted no contact and 1 denoted rigid contact. Four of the models – BALL, UNIVERSAL, HINGE and WELD – assumed that ground contact occurred at a single point under the foot: the CoP. In each of these models, the values of the weighting coefficients remained constant throughout the stance phase of gait, and so these models were categorised as time-independent. The remaining two models – SINGLEPOINT and MULTIPOINT – were categorised as time-dependent because the values of the weighting coefficients varied as a function of time to allow the foot to transition smoothly from heel-strike to foot-flat and from foot-flat to toe-off (see Figure 1). The SINGLEPOINT model assumed that ground contact occurred at a single point under the foot, the CoP, whereas the MULTIPOINT model assumed that the foot contacted the ground at five discrete points. Because foot-ground contact actually occurs over a finite surface area with varying kinematic constraints (Wojtyra 2003; Cheung and Zhang 2005), the MULTIPOINT model represented the most realistic model of foot-ground contact evaluated in this study.

A pseudo-inverse ground force decomposition method (Lin et al. 2011) was used to determine the contributions of all action forces to the vertical, fore-aft and mediolateral components of the GRF. At each instant of the gait cycle, each action force (e.g. a muscle force) obtained from the inverse dynamics analysis was applied in isolation to the model of the skeleton. A weighted least-squares optimisation problem was then solved to determine the contribution of each action force to the model-computed GRFs.

Superposition error was defined as the difference between the measured and computed GRFs. Superposition error was computed for each component of the GRF using a normalised root-mean-square error (NRMSE) approach. The NRMSE was found by calculating the RMS error of the difference between the measured GRF and the sum of all action force contributions to the model-computed GRF. This difference represents the accuracy of the rigid contact assumption imposed at each foot-ground contact point in the model (Anderson and Pandy 2003). A non-zero superposition error indicates that an additional external (fictitious) force must be applied to the foot to satisfy the rigid contact assumption. The RMS superposition error was normalised by the peak value of the measured GRF to obtain the NRMSE. The NRMSE was computed for each subject using all the six ground contact models and then averaged across all the subjects to obtain a mean NRMSE.

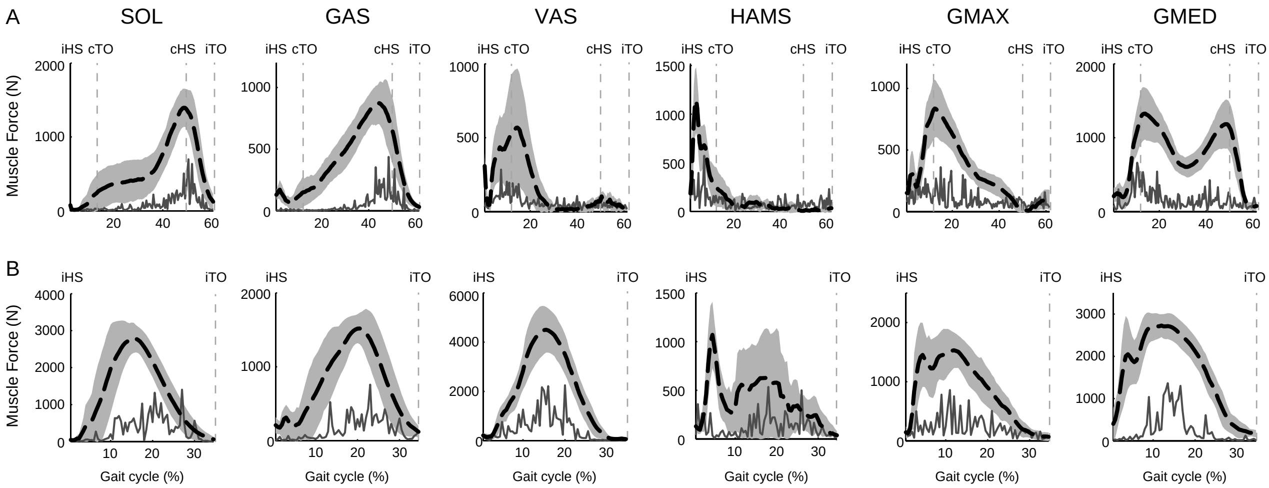

Figure 2. Muscle forces (dashed lines) calculated for walking (A) and running (B). The shaded regions represent ± 1 standard deviation from the mean. The wavy lines represent average muscle EMG data measured for the subjects. Muscle symbols: SOL (soleus), GAS (medial and lateral portions of GAS combined; medial GAS EMG shown), VAS (vastus medialis, vastus intermedius and vastus lateralis combined; vastus lateralis EMG shown), HAMS (medial and lateral portions of hamstrings combined; medial hamstring EMG shown), GMAX (gluteus maximus) and GMED (anterior and posterior portions of gluteus medius). Major gait events: iHS, ipsilateral heel-strike; iTO, ipsilateral toe-off; cHS, contralateral heel-strike; and cTO contralateral toe-off.

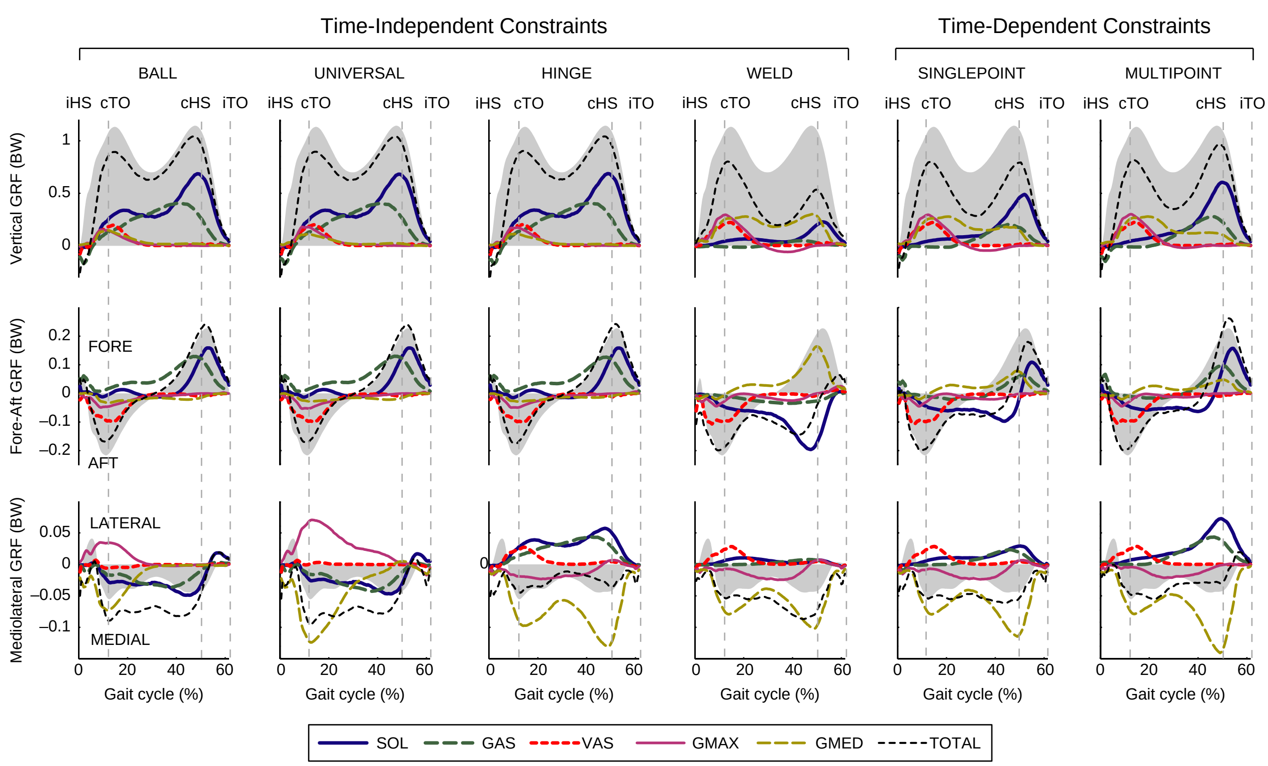

Figure 3. Muscle contributions to the vertical, fore-aft and mediolateral components of the GRF generated in walking. The shaded regions represent the forces recorded by the force plate. Results are shown for the six different ground contact models evaluated. The results for each contact model were averaged across all subjects. TOTAL represents the summed contributions of SOL, GAS, VAS, GMAX and GMED. Muscle symbols as defined in Figure 2. Forces are expressed in units of body weight (BW); the average mass of the subjects was 71.2 kg. Mediolateral ground forces are those represented for a right leg.

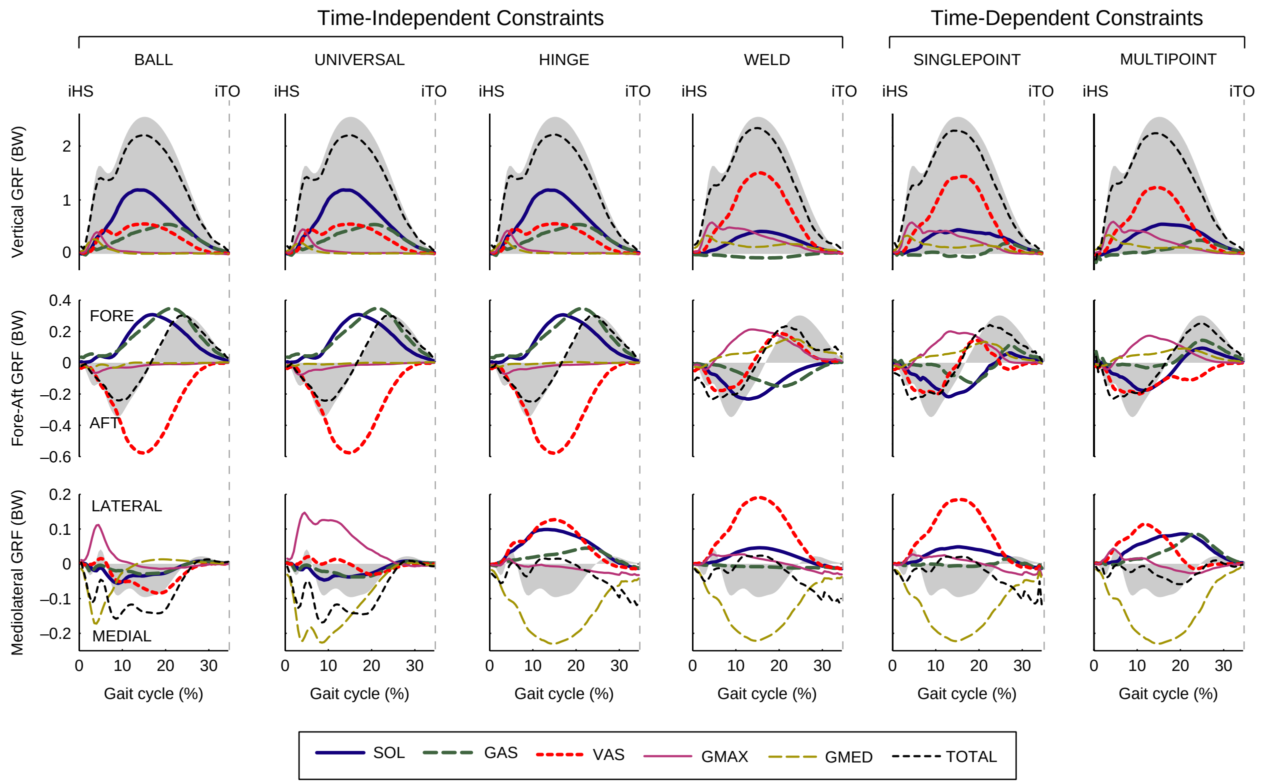

Figure 4. Muscle contributions to the vertical, fore-aft and mediolateral components of the GRF generated in running. The shaded regions represent the forces recorded by the force plate. Results are shown for the six different ground contact models evaluated. The results for each contact model were averaged across all subjects. TOTAL represents the summed contributions of SOL, GAS, VAS, GMAX and GMED. Muscle symbols as defined in Figure 2. Forces are expressed in units of BW; the average mass of the subjects was 71.2 kg. Mediolateral ground forces are those represented for a right leg.

Results

The timing of muscle contractions predicted for walking and running was similar to those exhibited by EMG signals measured during the experiment (Figure 2). The magnitudes of the muscle forces calculated for walking and running were also consistent with data reported previously by others (Anderson and Pandy 2001a; Thelen and Anderson 2006; Hamner et al. 2010).

In walking and running, five muscle groups – gluteus maximus (GMAX), gluteus medius (GMED), vasti (VAS), gastronemius (GAS) and soleus (SOL) – contributed most significantly to the vertical and fore-aft components of the GRF (Figures 3 and 4, TOTAL). The hamstrings (HAMS) and rectus femoris (RF) contributed relatively little (Tables 2 and 3).

Model estimates of muscle function were dependent on how foot-ground contact was modelled. For walking, the patterns of muscle function were similar in the vertical, fore-aft and mediolateral directions for the BALL and UNIVERSAL models. The HINGE model also predicted similar patterns of muscle function in the vertical and fore-aft directions; however, adding a kinematic constraint in the frontal plane (i.e. progressing from a UNIVERSAL joint to a HINGE joint) altered the actions of the GMAX and the ankle plantarflexors in the mediolateral direction (Figure 3 and Table 2). Adding another constraint in the sagittal plane (i.e. progressing from a HINGE joint to a WELD joint) changed the actions of the SOL in all three directions.

Model predictions of muscle function were also influenced by the presence of time-dependent kinematic constraints in the ground-contact model. For walking, the contributions of the ankle plantarflexors to the vertical ground force were reduced in the first half of stance for the SINGLEPOINT and MULTIPOINT models (Figure 3). These models also showed that the ankle plantarflexors accelerated the centre of mass in late stance, contrary to the behaviour predicted by the WELD model.

For running, the SOL generated the majority of support during stance when the BALL, UNIVERSAL and HINGE models were used to simulate ground contact, whereas the VAS contributed most significantly to support when the WELD, SINGLEPOINT and MULTIPOINT models were used (Figure 4 and Table 3). Whereas the SINGLEPOINT and MULTIPOINT models predicted similar patterns of muscle coordination for walking, differences were evident in the coordination predicted for running, particularly in

Table 2. Peak contributions of muscle forces and gravitational forces (gravity) to the vertical, fore-aft and mediolateral GRFs generated in walking.

		BALL			UNIVERSAL			HINGE			WELD			SINGLEPOINT			MULTIPOINT		
		Foreaft	Vert	MedLat	Foreaft	Vert	MedLat	Foreaft	Vert	MedLat	Foreaft	Vert	MedLat	Foreaft	Vert	MedLat	Foreaft	Vert	MedLat
GMAX	Mean	−0.06	0.18	0.05	−0.06	0.21	0.06	−0.06	0.20	−0.03	−0.04	0.31	−0.03	−0.05	0.31	−0.03	−0.05	0.32	−0.02
	STD	0.02	0.06	0.03	0.03	0.06	0.05	0.03	0.06	0.02	0.05	0.13	0.02	0.04	0.14	0.02	0.04	0.14	0.03
GMED	Mean	−0.04	0.18	−0.08	−0.04	0.16	−0.13	−0.04	0.16	−0.14	0.17	0.36	−0.11	0.11	0.35	−0.12	0.04	0.32	−0.14
	STD	0.02	0.10	0.04	0.02	0.09	0.04	0.02	0.10	0.03	0.06	0.09	0.02	0.09	0.09	0.03	0.05	0.08	0.04
ILPSO	Mean	0.03	−0.05	0.02	0.03	−0.05	0.01	0.02	−0.06	0.04	0.25	0.38	0.07	0.17	0.27	0.05	0.07	0.05	0.03
	STD	0.04	0.09	0.02	0.04	0.09	0.03	0.05	0.10	0.03	0.12	0.26	0.04	0.11	0.25	0.04	0.07	0.25	0.04
HAMS	Mean	0.06	0.17	0.02	0.06	0.18	0.02	0.06	0.19	−0.01	0.12	0.02	−0.02	0.10	0.11	−0.02	0.08	0.13	−0.02
	STD	0.01	0.07	0.02	0.01	0.07	0.02	0.02	0.08	0.02	0.04	0.13	0.02	0.04	0.13	0.02	0.03	0.11	0.02
RF	Mean	−0.07	0.15	−0.01	−0.07	0.15	−0.01	−0.07	0.15	−0.02	0.05	0.29	−0.01	−0.07	0.18	−0.02	−0.08	0.17	−0.03
	STD	0.05	0.04	0.02	0.06	0.04	0.01	0.06	0.04	0.01	0.08	0.10	0.02	0.05	0.08	0.01	0.02	0.06	0.01
VAS	Mean	−0.12	0.24	−0.01	−0.12	0.25	−0.01	−0.12	0.24	0.02	−0.14	0.24	0.02	−0.13	0.22	0.02	−0.13	0.20	0.03
	STD	0.07	0.11	0.02	0.07	0.12	0.02	0.07	0.14	0.03	0.05	0.18	0.03	0.06	0.20	0.03	0.05	0.23	0.02
GAS	Mean	0.14	0.38	−0.05	0.14	0.38	−0.05	0.14	0.39	0.05	−0.04	0.05	0.00	0.11	0.11	0.02	0.12	0.27	0.05
	STD	0.03	0.26	0.04	0.03	0.26	0.05	0.03	0.26	0.01	0.01	0.04	0.01	0.05	0.31	0.03	0.04	0.21	0.01
SOL	Mean	0.18	0.73	−0.04	0.18	0.72	−0.04	0.17	0.73	0.06	−0.21	0.26	0.00	−0.02	0.54	0.03	0.14	0.65	0.08
	STD	0.04	0.10	0.07	0.04	0.10	0.07	0.04	0.10	0.03	0.03	0.07	0.03	0.19	0.24	0.03	0.12	0.13	0.02
Gravity	Mean	−0.04	0.25	0.02	−0.04	0.26	0.02	−0.05	0.27	0.02	0.05	0.32	0.03	0.02	0.30	0.02	−0.07	0.31	0.02
	STD	0.02	0.03	0.03	0.02	0.03	0.02	0.02	0.03	0.01	0.11	0.03	0.01	0.10	0.03	0.01	0.05	0.04	0.02

Data were averaged across all subjects. STD represents ± one standard deviation from the mean. All data are expressed in units of BW (subjects' average mass = 71.2 kg). Muscle symbols as defined in Figure 2. ILPSO, iliacus and psoas combined; RF, rectus femoris.

Table 3. Peak contributions of muscle forces and gravitational forces (gravity) to the vertical, fore-aft and mediolateral GRFs generated in running.

		BALL			UNIVERSAL			HINGE			WELD			SINGLEPOINT			MULTIPOINT		
		Foreaft	Vert	MedLat	Foreaft	Vert	MedLat	Foreaft	Vert	MedLat	Foreaft	Vert	MedLat	Foreaft	Vert	MedLat	Foreaft	Vert	MedLat
GMAX	Mean	−0.07	0.41	0.07	−0.08	0.46	0.12	−0.07	0.44	−0.05	0.16	0.56	−0.04	0.16	0.56	−0.04	0.13	0.57	0.00
	STD	0.04	0.13	0.10	0.06	0.15	0.09	0.05	0.13	0.04	0.12	0.23	0.06	0.11	0.23	0.06	0.12	0.24	0.06
GMED	Mean	−0.04	0.29	−0.18	−0.02	0.25	−0.24	−0.03	0.28	−0.21	0.14	0.35	−0.21	0.12	0.35	−0.21	0.09	0.36	−0.21
	STD	0.06	0.10	0.06	0.05	0.09	0.08	0.05	0.10	0.06	0.07	0.12	0.05	0.07	0.12	0.05	0.05	0.12	0.05
ILPSO	Mean	0.05	−0.09	0.01	0.05	−0.09	0.01	0.05	−0.10	−0.01	0.01	−0.22	−0.03	−0.03	−0.21	−0.03	0.02	−0.19	0.01
	STD	0.06	0.16	0.03	0.06	0.17	0.03	0.06	0.18	0.03	0.18	0.23	0.04	0.15	0.22	0.04	0.10	0.20	0.04
HAMS	Mean	0.09	−0.01	0.01	0.10	−0.01	0.00	0.10	−0.02	−0.03	0.13	0.01	−0.03	0.13	0.04	−0.03	0.13	0.01	0.00
	STD	0.04	0.11	0.03	0.04	0.11	0.03	0.04	0.11	0.02	0.05	0.12	0.03	0.04	0.11	0.03	0.04	0.13	0.03
RF	Mean	−0.16	0.18	−0.04	−0.17	0.19	−0.01	−0.17	0.19	−0.04	−0.18	0.22	−0.04	−0.18	0.21	−0.04	−0.18	0.19	−0.03
	STD	0.05	0.04	0.02	0.05	0.03	0.03	0.05	0.03	0.02	0.06	0.04	0.02	0.06	0.04	0.02	0.06	0.04	0.01
VAS	Mean	−0.49	0.51	−0.05	−0.49	0.51	0.00	−0.49	0.52	0.11	−0.06	1.23	0.16	−0.19	1.19	0.15	−0.28	1.06	0.08
	STD	0.21	0.25	0.10	0.21	0.25	0.09	0.22	0.25	0.06	0.21	0.63	0.08	0.24	0.59	0.08	0.18	0.54	0.13
GAS	Mean	0.31	0.54	−0.02	0.31	0.54	−0.02	0.31	0.55	0.04	−0.09	−0.04	−0.01	0.13	0.27	0.01	0.17	0.18	0.10
	STD	0.09	0.32	0.08	0.09	0.32	0.09	0.09	0.34	0.05	0.14	0.20	0.04	0.20	0.32	0.05	0.11	0.34	0.05
SOL	Mean	0.29	1.20	−0.02	0.29	1.20	−0.02	0.29	1.20	0.11	−0.16	0.53	0.05	−0.13	0.67	0.06	−0.14	0.72	0.12
	STD	0.06	0.37	0.13	0.06	0.37	0.12	0.06	0.37	0.03	0.21	0.13	0.05	0.23	0.32	0.05	0.20	0.26	0.04
Gravity	Mean	0.00	0.25	0.02	0.00	0.25	0.01	0.00	0.27	−0.01	0.10	0.30	0.01	0.02	0.28	0.00	0.01	0.29	0.02
	STD	0.08	0.04	0.03	0.08	0.04	0.03	0.08	0.02	0.03	0.09	0.03	0.03	0.09	0.03	0.03	0.08	0.03	0.02

Data were averaged across all subjects. STD represents ± one standard deviation from the mean. All data are expressed in units of BW (subjects' average mass = 71.2 kg). Muscle symbols as defined in Figure 2. ILPSO, iliacus and psoas combined; RF, rectus femoris.

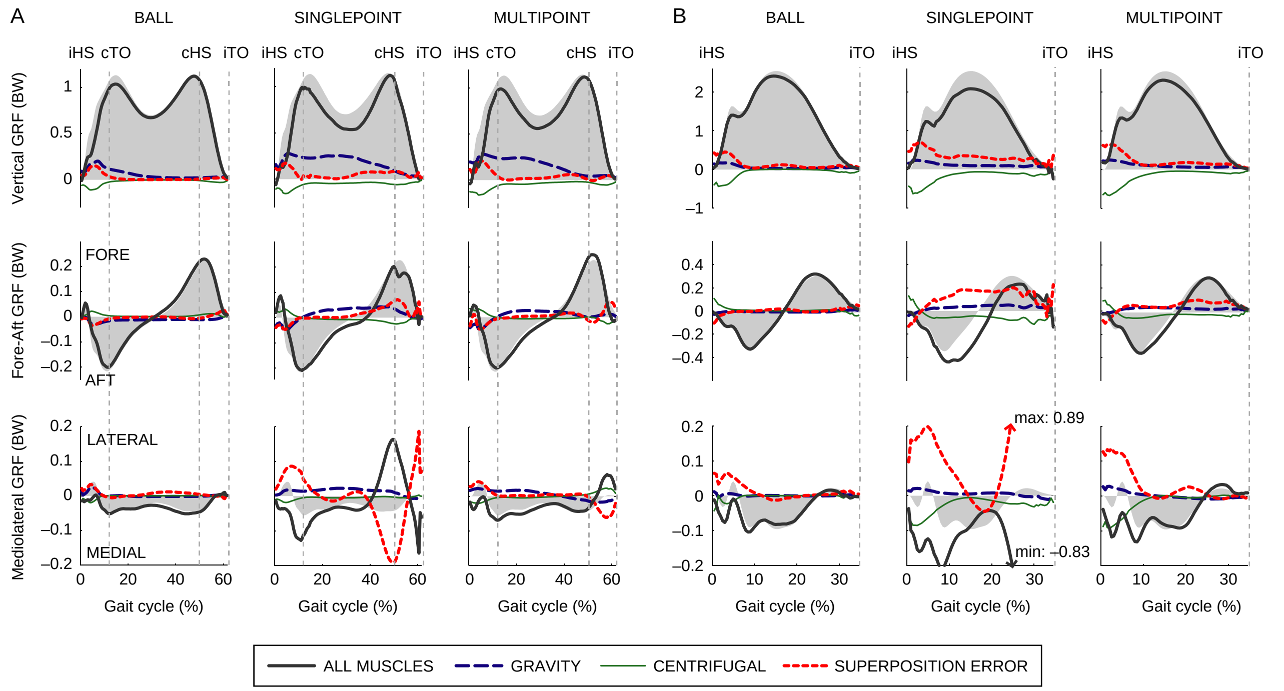

Figure 5. Contributions of all muscle forces (all muscles), gravitational forces (gravity) and centrifugal and Coriolis forces (centrifugal) to the vertical, fore-aft and mediolateral components of the GRFs generated in walking (A) and running (B). The shaded regions represent the forces recorded by the force plate. Superposition error was found by subtracting the model-computed GRF (i.e. All muscles, gravity and centrifugal summed together) from the measured GRF. Results are shown for three different ground contact models for each gait. The results for each contact model were averaged across all subjects. Forces are expressed in units of BW; the average mass of the subjects was 71.2 kg. Mediolateral ground forces are those represented for a right leg.

the mediolateral direction (Figures 3 and 4, compare VAS and GAS). Calculations of muscle function in the mediolateral direction were most sensitive to the way in which foot-ground contact was modelled.

Superposition error was sensitive to both gait speed and the model used to simulate foot-ground contact (Figures 5 and 6). The errors for running were larger than those for walking. Superposition errors were largest for the HINGE, WELD and SINGLEPOINT models, and they were also larger in the mediolateral direction than the vertical and fore-aft directions (Figure 6(A) and (B)). In running, for example, the HINGE, WELD and SINGLE-POINT models generated errors that were three times greater than the peak GRF measured in the mediolateral direction. The total superposition errors for the BALL, UNIVERSAL, HINGE and WELD models increased as the number of degrees of freedom of the foot-ground contact model decreased (Figure 6(C)).

Discussion

Calculations of muscle coordination in human gait are influenced by the model used to simulate foot-ground contact. Two factors – the number of foot-ground contact points assumed in the model and the type of kinematic constraint enforced at each contact point – can significantly alter the model predictions of muscle function for both walking and running.

Kinematic constraints act at each of the foot-contact points to restrict the motion of the foot and alter the calculated values of the muscle contributions to the GRFs generated in walking and running (Figures 3 and 4). Our results indicate, first, that kinematic constraints applied in the sagittal plane affect the model calculations of muscle contributions to the vertical and fore-aft GRFs; second, that kinematic constraints applied in the frontal plane affect the calculations of muscle contributions to the mediolateral GRF; and third, that kinematic constraints applied in the transverse plane have little effect on the model calculations of muscle function.

Estimates of leg-muscle function are also influenced by the number of foot-contact points included in the model. Muscle contributions to the vertical and fore-aft GRFs were found to be similar for the SINGLEPOINT and MULTIPOINT models. The results obtained from these two models are consistent with the findings of Liu et al. (2008), who used a single contact point to simulate the interaction between the foot and the ground during walking, and with those of Sasaki and Neptune (2006), who used a more complex model comprising 30 foot-springs distributed over the sole of the foot to simulate both walking and running. These findings suggest that

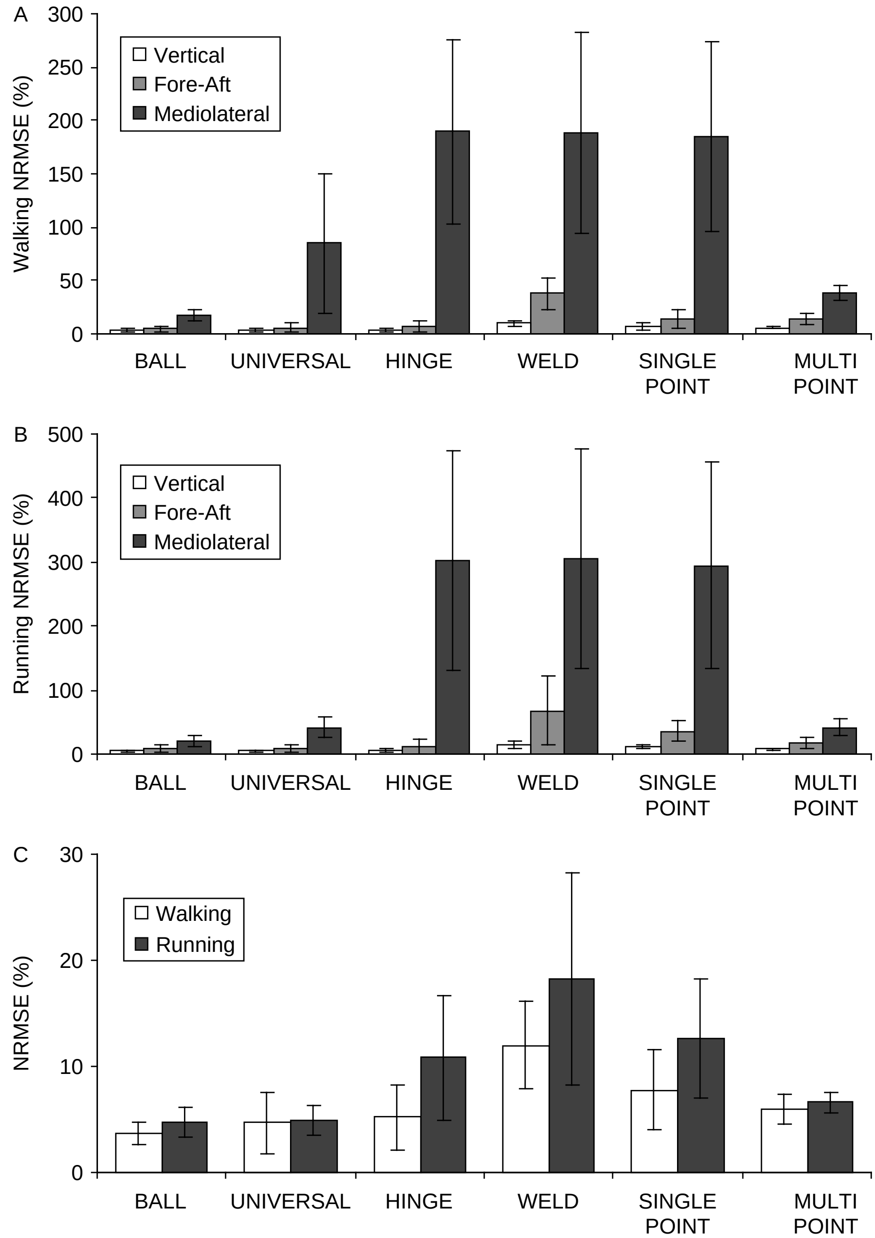

Figure 6. Normalised root mean square errors (NRMSE) calculated for the vertical, fore-aft and mediolateral components of the GRF generated in walking (A) and running (B). NRMSE was found by subtracting the model-computed GRF from the measured GRF and then normalising by the peak value of the measured GRF (see text). The error bars indicate ± one standard deviation from the mean. (C) Total NRMSE calculated for walking and running. Total NRMSE was found by performing a vector summation of the NRMSE values calculated for the vertical, fore-aft and mediolateral directions shown in (A) and (B) above.

predictions of muscle function in the sagittal plane are insensitive to the number of foot-contact points included in the model, provided that foot motion is adequately constrained. In contrast, muscle contributions to the mediolateral ground force were different for the SINGLEPOINT and MULTIPOINT models (Figures 3, 4 and 6), indicating that calculations of muscle function in the mediolateral direction are sensitive to the number and location of foot-contact points included in the model.

Different models of ground contact may also yield conflicting predictions of muscle function during gait. In walking, the VAS and SOL support the skeleton in early and late stance, respectively, whereas in running, these muscles act in unison to provide a greater upward acceleration of the centre of mass (Sasaki and Neptune 2006; Pandy and Andriacchi 2010). At running speeds similar to that adopted in this study, Hamner et al. (2010) used the UNIVERSAL contact model and found the contribution of SOL to be twice that of VAS, whereas Pandy and Andriacchi (2010) used the MULTIPOINT model and obtained the opposite result (i.e. the force of VAS contributed twice as much as the force of SOL to the vertical GRF). This contradictory result is likely due to (1) differences in musculoskeletal model architecture, and (2) different models of foot-ground contact. With regard to the musculoskeletal model, many factors can influence the simulated activation of the VAS and SOL muscles (e.g. moment arm, maximum isometric strength, optimal fibre length), and hence effect their relative contribution to the ground reaction force in gait. However, the present study illustrates nevertheless that vastly different functions may be predicted for VAS and SOL when using different ground contact models, despite employing the same musculoskeletal model and muscle forces across all trials (Figure 4, compare results for the UNIVERSAL and MULTIPOINT models in the vertical direction.) Our results show that VAS generates the majority of the vertical GRF when the sagittal plane rotational kinematic constraint is enforced, whereas SOL dominates when this constraint is removed (see Table 1). To our knowledge, the studies by Hamner et al. (2010) and Pandy and Andriacchi (2010) are the only ones to have evaluated muscle-induced accelerations at running speeds above 3 m/s. The inconsistent results obtained from these studies highlight the need for future work aimed at validating model predictions of leg-muscle function in walking and running.

Lower superposition errors do not necessarily imply greater validity in the predictions of leg-muscle function. The BALL contact model permitted foot movement about all three axes of rotation (Table 1) (i.e. kinematic constraints were not enforced about any joint axis), which resulted in a superposition error lower than that obtained from any of the other models (Figure 6). The MULTIPOINT contact model produced a similar superposition error to that calculated in the BALL model, yet the predictions of individual muscle function obtained from these models were significantly different (Figures 3 and 4). These differences are attributed to the differences in the kinematic constraints acting at the points of contact between the foot and the ground, which change the equations of motion and influence the calculations of muscle function. Superposition error only quantifies the accuracy with which the various action forces sum to the total GRF; it does not verify the calculations of the contributions of the individual action forces themselves.

Model predictions of muscle function have not been validated by experiment because muscle contributions to the GRF are difficult to measure. However, Hunter et al. (2009) measured the induced hip- and knee-joint angular accelerations by electrically stimulating individual muscles in a range of postures during the swing phase of walking. In a similar fashion, one could electrically stimulate a single muscle and measure the resulting GRF. Experiments such as these would be valuable in evaluating the suitability of different ground contact models in calculations of leg-muscle function during gait.

This study is limited in at least three respects. First, the same musculoskeletal model was used to simulate both walking and running in all subjects. Although body-segment parameters were scaled according to each subject's anthropometry, the same muscle-tendon properties were assumed for all subjects, which may have influenced the calculated values of muscle forces and hence the model predictions of muscle function. Second, the present analysis was limited to self-selected speeds of walking and running that were characterised by initial heel impact. As running speed increases, foot-ground contact occurs at more anterior positions on the foot, and is located wholly on the toes during maximal sprinting (Nett 1964; Novacheck 1998). The MULTIPOINT model formulated in this study has the advantage that it may be used to simulate any form of running, including toe-running, because the kinematic constraints acting between the foot and the ground are governed by the location of the CoP, which can be measured accurately in a gait-analysis experiment. Third, relatively large superposition errors were observed close to heel-strike in all ground contact models, particularly in the mediolateral direction (Figures 5 and 6). This may have been caused by small linear translations of the foot relative to the ground during impact. Though these translations may be small in life, they were not permitted in any of the contact models evaluated here. Future work should, therefore, be directed towards incorporating a more detailed representation of collision mechanics into existing models of foot-ground contact.

As ground-force decomposition analyses become more widespread (Delp et al. 2007), careful consideration should be given to the formulation of the model used to simulate ground contact. The results of this study show that model calculations of muscle contributions to the GRF, particularly the component in the mediolateral direction, are sensitive to the distribution of foot-contact points and the type of kinematic constraint used to model the interaction between the foot and the ground. These findings have important implications for analyses of leg-muscle function in gait, particularly if the results of such analyses are to guide clinical decision making.

Acknowledgements

We thank Dr Anthony Schache and Doug Rosemond for their help with experimental data collection. This work was supported by a VESKI Innovation Fellowship and Australian Research Council Discovery Grants DP0772838 and DP0878705.

References

Anderson FC, Pandy MG. 1999. A dynamic optimization solution for vertical jumping in three dimensions. Comput Methods Biomech Biomed Engin. 2(3):201–231.

Anderson FC, Pandy MG. 2001a. Dynamic optimization of human walking. J Biomech Eng. 123(5):381–390.

Anderson FC, Pandy MG. 2001b. Static and dynamic optimization solutions for gait are practically equivalent. J Biomech. 34(2):153–161.

Anderson FC, Pandy MG. 2003. Individual muscle contributions to support in normal walking. Gait and Posture. 17(2):159–169.

Arnold AS, Anderson FC, Pandy MG, Delp SL. 2005. Muscular contributions to hip and knee extension during the single limb stance phase of normal gait: a framework for investigating the causes of crouch gait. J Biomech. 38(11):2181–2189.

Cheung JT, Zhang M. 2005. A 3-dimensional finite element model of the human foot and ankle for insole design. Arch Phys Med Rehabil. 86(2):353–358.

Delp SL, Anderson FC, Arnold AS, Loan P, Habib A, John CT, Guendelman E, Thelen DG. 2007. OpenSim: open-source software to create and analyze dynamic simulations of movement. IEEE Trans Biomed Eng. 54(11):1940–1950.

Goldberg S, Kepple TM. 2009. Muscle-induced accelerations at maximum activation to assess individual muscle capacity during movement. J Biomech. 42(7):952–955.

Hamner SR, Seth A, Delp SL. 2010. Muscle contributions to propulsion and support during running. J Biomech. 43(14): 2709–2716 .

Hunter BV, Thelen DG, Dhaher YY. 2009. A three-dimensional biomechanical evaluation of quadriceps and hamstrings function using electrical stimulation. IEEE Trans Neural Syst Rehabil Eng. 17(2):167–175.

Kepple TM, Siegel KL, Stanhope S. 1997a. The use of two foot-floor models to examine the role of the ankle plantarflexors in the forward acceleration of normal gait. Gait and Posture. 5(2):172–173.

Kepple TM, Siegel KL, Stanhope SJ. 1997b. Relative contributions of the lower extremity joint moments to forward progression and support during gait. Gait and Posture. 6(1):1–8.

Kim HJ, Fernandez JW, Akbarshahi M, Walter JP, Fregly BJ, Pandy MG. 2009. Evaluation of predicted knee-joint muscle forces during gait using an instrumented knee implant. J Orthop Res. 27(10):1326–1331.

Li X, Zhou P, Aruin AS. 2007. Teager–Kaiser energy operation of surface EMG improves muscle activity onset detection. Ann Biomed Eng. 35(9):1532–1538.

Lin YC, Kim HJ, Pandy MG. 2011. A computationally efficient method for assessing muscle function during human locomotion. Int J Numer Method Biomed Eng. 27:436–449.

Liu MQ, Anderson FC, Schwartz MH, Delp SL. 2008. Muscle contributions to support and progression over a range of walking speeds. J Biomech. 41(15):3243–3252.

Neptune RR, Wright IC, Van Den Bogert AJ. 2000. A method for numerical simulation of single limb ground contact events: application to heel-toe running. Comput Methods Biomech Biomed Engin. 3(4):321–334.

Nett T. 1964. Foot plant in running. Track Tech. 15:462–463.

Novacheck TF. 1998. The biomechanics of running. Gait and Posture. 7(1):77–95.

Pandy MG, Andriacchi TP. 2010. Muscle and joint function in human locomotion. Annu Rev Biomed Eng. 12:401–433.

Pandy MG, Lin YC, Kim HJ. 2010. Muscle coordination of mediolateral balance in normal walking. J Biomech. 43(11): 2055–2064.

Reinbolt JA, Schutte JF, Fregly BJ, Koh BI, Haftka RT, George AD, Mitchell KH. 2005. Determination of patient-specific multi-joint kinematic models through two-level optimization. J Biomech. 38(3):621–626.

Sasaki K, Neptune RR. 2006. Differences in muscle function during walking and running at the same speed. J Biomech. 39(11):2005–2013.

Thelen DG, Anderson FC. 2006. Using computed muscle control to generate forward dynamic simulations of human walking from experimental data. J Biomech. 39(6):1107–1115.

Wojtyra M. 2003. Multibody simulation model of human walking. Mech Based Design Struct Mach. 31(3):357–379.

Xiao M, Higginson JS. 2008. Muscle function may depend on model selection in forward simulation of normal walking. J Biomech. 41(15):3236–3242.

Zajac FE, Gordon ME. 1989. Determining muscle's force and action in multi-articular movement. Exerc Sport Sci Rev. 17:187–230.